Next-Generation Air–Ocean–Wave Coupled Ocean/Atmosphere Mesoscale Prediction System (COAMPS)

S. Chen,[1] T.J. Campbell,[2] S. Gaberšek,[3] H. Jin,[1]
and R.M. Hodur[4]
[1]*Marine Meteorology Division*
[2]*Oceanography Division*
[3]*University Corporation for Atmospheric Research*
[4]*SAIC, Monterey, California*

Introduction: A team of NRL scientists from the Marine Meteorology and Oceanography Divisions has successfully transformed the one-way air–ocean Coupled Ocean/Atmosphere Mesoscale Prediction System (COAMPS®*) into a six-way fully coupled air–ocean–wave weather and marine forecasting system. This was accomplished using the state-of-the-art Earth System Modeling Framework (ESMF), making COAMPS the first limited area model to utilize ESMF in an effort to seamlessly couple multiple, individually skillful models into one flexible, coherent modeling system. The components used here consist of the COAMPS atmospheric model, the Navy Coastal Ocean Model (NCOM), two interchangeable wave models — Simulating WAves Nearshore (SWAN) and WAVEWATCH III — and a new air–sea coupler developed at NRL that surmounted many of the technical challenges that arose during the development of the coupled system. A mechanism was implemented in the air–sea coupler to support interoperable inter-exchange of two different wave models and different wave feedbacks to the ocean and atmosphere, a feature that enhances the capability of the coupled system to adapt new components. Additionally, special atmospheric, ocean, and wave hurricane observations were obtained to investigate and validate the sensitivity of hurricane intensity and track change in the forecast system due to various coupling processes.

Coupling Methods: A fully coupled air–sea–wave model can provide a natural mechanism for frequent two-way feedback between the air–ocean, air–wave, and ocean–wave components. Figure 1 shows the variety of model variables that are exchanged between each set of coupled components over the course of the coupled time-step. As illustrated in the figure, the atmospheric component provides a total of six ocean surface boundary forcing fields to the ocean component, while the ocean model returns a new sea surface temperature to the atmosphere that influences the next time-step prediction of the atmospheric surface fluxes

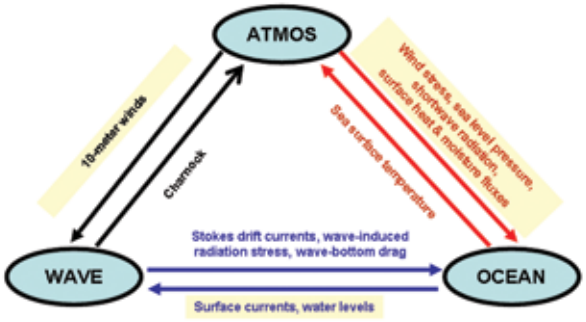

FIGURE 1
A schematic diagram of COAMPS six-way coupling between the atmospheric, ocean, and wave models and the fields that are exchanged between each pair of components.

and wind stress. The ocean component also provides the current and sea surface height to the wave component, while the atmospheric component impacts the waves through the wind-driven momentum drag. The feedback of the wave component to the ocean consists of 10 forcing terms, including the Stokes drift current, wave radiation stress gradients, wave-bottom current, and wave-bottom current radian frequency. The wave component feedback to the atmosphere consists of a nondimensional roughness length (Charnock number), which is related to the atmospheric momentum drag.

Hurricane Forecast Assessment: The prestorm ocean conditions, such as the warm or cold eddies along a hurricane track, influence the rapid intensity change of a hurricane. Additionally, a hurricane can induce a trailing ocean cold wake anomaly (up to several

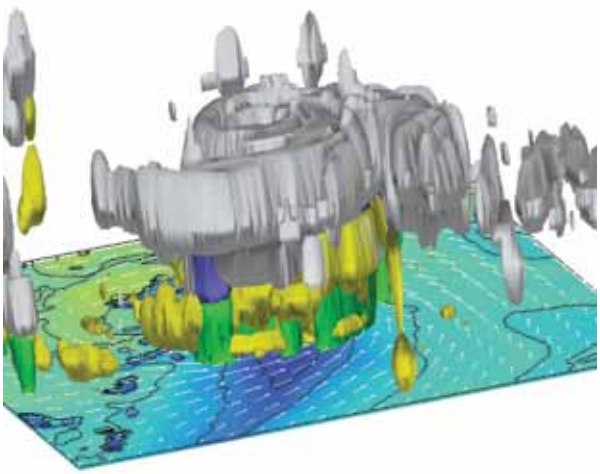

FIGURE 2
Six-way coupled COAMPS 48-h simulation of Hurricane Frances (2004). The figure shows the 0.1 kg/kg isosurface plots of cloud (yellow), ice (white), rain (green), and graupel (purple) mixing ratio. The color shading is the sea surface temperature with darker shade of blue depicting the cooling beneath the hurricane. The white arrows represent the 10-m wind (m/s). The view is from the southeast flank of the storm.

*COAMPS is a registered trademark of the Naval Research Laboratory.

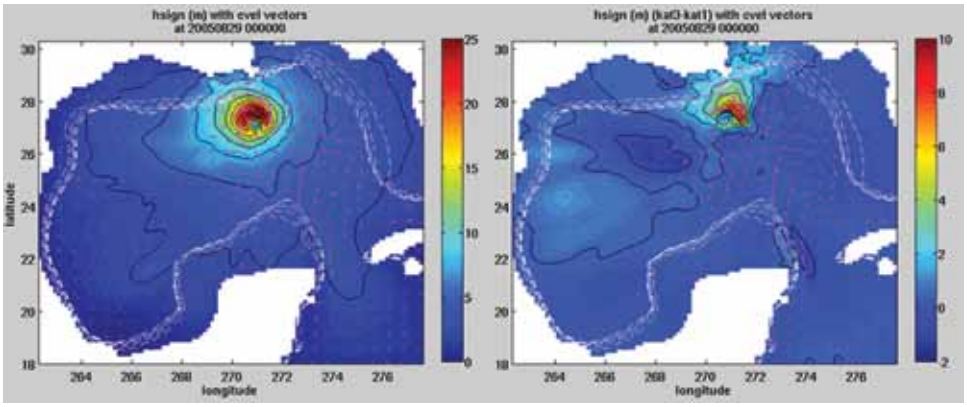

FIGURE 3
Comparisons of COAMPS simulated Hurricane Katrina (2005) significant wave height (m) without the currents forcing in the SWAN wave model (left panel) and the significant wave height difference between the run with the current and the run without the current (right panel). The red arrows are the surface currents. Note that the wave heights in the front right quadrant of the storm are reduced in this five-way coupled run. This is the result of currents being in the same direction of the surface wave packet propagation, which tends to increase the wave packet speed and decreases the wave heights.

degrees) that tends to form preferentially to the right of the storm track and can extend hundreds of kilometers to the rear of the storm, shown by our 48-h simulation in Fig. 2. This intriguing feature is important both for its immediate impact on the storm evolution as well as longer-term climatic impacts to changes in the ocean heat storage below the thermocline. To examine the impact of this feature on the tropical cyclone (TC) simulation in the model, the team performed a series of runs to evaluate the impact of coupling vs no coupling on two mature category 4 and 5 hurricanes, Katrina (2005) and Frances (2004). We compared the atmospheric model prediction of the hurricane track, intensity, and gale force wind radii; the ocean model prediction of the hurricane-induced cold ocean wake; and the surface wave model prediction of the significant wave height and period with the available observations. Among the most important findings are the following. First, two-way air–ocean coupling developed a cold ocean wake that acted to reduce the intensity of the simulated storm. This weakening was manifested by an increased asymmetry in the hurricane secondary circulation and expansion of the eye wall. Second, it was discovered that the horizontal advection of the near-surface cold ocean water contributed to the upper-ocean cooling and weakening of the hurricane as much as the vertical mixing and upwelling.[1] These new results show that the magnitude and size of the trailing ocean cold wake cannot be fully represented by coupling with simple one-dimensional mixed layer models only. Third, including the ocean current and water level forcing in the wave model reduced the hurricane-induced significant wave height bias in the front right quadrant of the storm (Fig. 3). This may have important implications for improving the maximum forecasted surge heights that tend to be found in this quadrant of the storm. Finally, the 48-h intensity and track differences between the uncoupled and various coupled runs (one-to six-way coupling) were found to be as large as 18 m/s and 10 nautical miles, respectively. Further experiments are required to determine if this is typical for other tropical cyclones that form in other parts of the world as well.

Summary and Conclusions: Validation of the two-way coupling between the atmosphere and ocean only also showed forecast improvements in a variety of non-hurricane atmosphere and ocean phenomena.[2] With the new coupling capability in COAMPS, NRL scientists can now conduct a wider range of new research applications to further the understanding of the air–sea interaction processes that are of the utmost importance to the Navy.

Acknowledgments: We thank Dr. Melinda Peng, Dr. Jerome Schmidt, Dr. Travis Smith, Mr. Rick Allard, and Mr. Eric Rogers for discussions; and Drs. Paul Martin and James Doyle for providing the surface wave-current and surface wave-wind feedback algorithms.

[Sponsored by the DoD High Performance Computing Modernization Program]

References

[1] S. Chen, T.J. Campbell, H. Jin, S. Gaberšek, R.M. Hodur, and P. Martin, "Effect of Two-way Air–Sea Coupling in High and Low Wind Speed Regimes," *Mon. Wea. Rev.* **138**, 3579–3602 (2010).

[2] R.A. Allard, T.J. Campbell, R.J. Small, T.A. Smith, T.G. Jensen, S. Chen, J.A. Cummings, J.D. Doyle, X. Hong, and S.N. Carroll, "Validation Test Report for the Coupled Ocean Atmospheric Mesoscale Prediction System (COAMPS), Version 5," NRL/MR/7322--10-9283, Naval Research Laboratory, (2010).

New Ocean Wind Capability from Space

T.F. Lee,[1] M.H. Bettenhausen,[2] and J.D. Hawkins[1]
[1] *Marine Meteorology Division*
[2] *Remote Sensing Division*

Introduction: WindSat is a satellite-based polarimetric microwave radiometer designed and developed by the Naval Research Laboratory Remote Sensing Division and the Naval Center for Space Technology.[1] WindSat was launched in 2003 to demonstrate the capability of polarimetric microwave radiometry to measure the ocean surface wind vector from space. This demonstration has been highly successful, enabling WindSat data to be used operationally for weather forecasting (for example, to monitor tropical cyclone structure worldwide) and as input to numerical weather prediction models of the U.S. Navy, the U.S. National Oceanic and Atmospheric Administration (NOAA), and the United Kingdom Met Office.

The NRL WindSat ocean retrieval algorithm is an optimal estimation algorithm for retrieving the ocean surface wind vector and sea surface temperature from WindSat measurements.[2] The WindSat measurements represent a combination of microwave energy emitted and reflected from the Earth's surface and absorption and emission of the microwave energy as it propagates through the atmosphere. The algorithm also retrieves columnar atmospheric water vapor and columnar atmospheric cloud liquid water (CLW). We use a physically based forward model for the WindSat measurements that couples a one-layer atmospheric model with a sea surface emissivity model that accounts for wind-induced roughness and sea surface foam. The optimization algorithm adjusts the retrieved parameters to match the WindSat measurements. Near-real-time examples of WindSat products appear at http://www.nrl.navy.mil/WindSat/.

Forecasting Case Examples: Figure 4, which shows a cold front off the west coast of the U.S., illustrates the characteristic shift of winds from the southwest equatorward of a cold frontal band (white) to northwest poleward of the frontal band. Wind speeds (WS) throughout the image are generally from 20 to 30 kt with some higher speeds in the vicinity of the front. The convergence of winds along the front is, in part, what produces the upward motion responsible for the cloud band. Shades of gray indicate vertically integrated quantities of CLW from 0.0 (black) to 0.5 mm (white). White values without overplotted vectors indicate unavailable retrievals due to precipitation. Where black vectors are plotted on top of white, retrievals should be examined more closely for consistency. Similar retrievals are assimilated into numerical weather prediction models.

WindSat wind plots are used routinely by a variety of responsible agencies for routine reconnaissance of tropical cyclones. While heavy rain and clouds often prevent wind retrieval of the strongest winds near the central core of storms, useful wind information is still often observed in adjacent areas. Figure 5, which shows the WindSat vectors derived from Hurricane Earl, shows near-hurricane force winds of approximately 60 kt near the storm center in a large cloud-free (nearly black) region. While CLW amounts are too great for wind retrieval over most of the interior of the storm

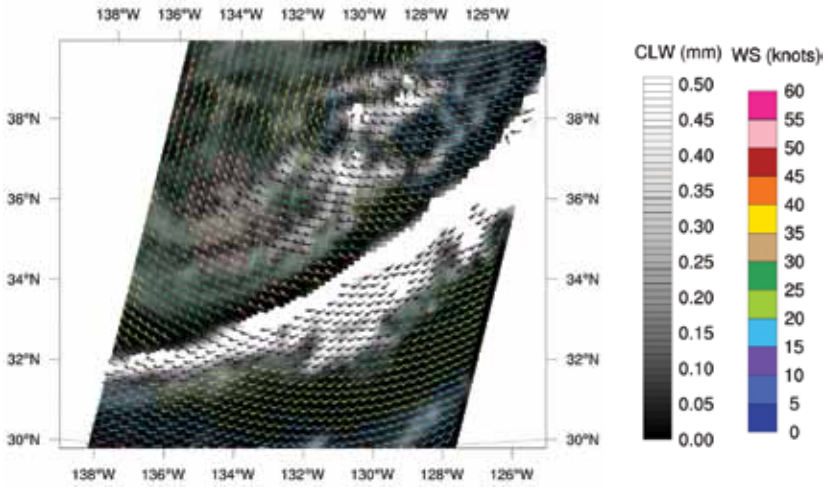

FIGURE 4
Frontal system off California, December 29, 2003. White indicates potential rain contamination of vector accuracy. Colored vectors show wind speed and direction; black vectors should be examined further for reliability.

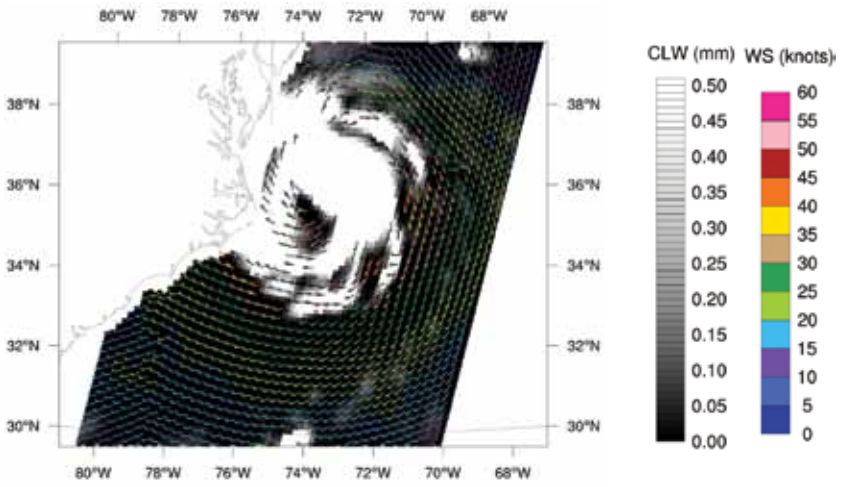

FIGURE 5
Hurricane Earl off the east coast of the United States, September 3, 2010. White indicates potential rain contamination of vector accuracy.

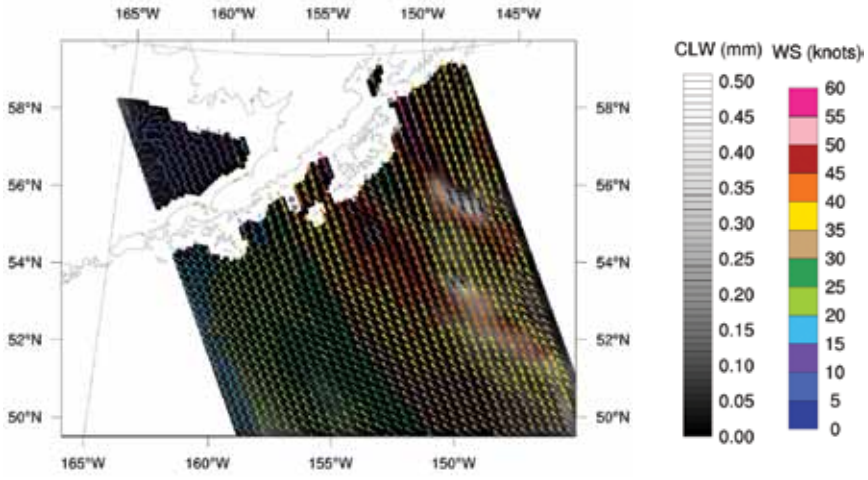

FIGURE 6
Gap winds south of Alaska, November 30, 2010.

(white without vectors), on the periphery of the storm where CLW is absent or reduced (black or gray), the vectors reveal a counterclockwise circulation. Remotely sensed winds from hurricane hunter airplane flights observed at nearly the same time show a strong correspondence to the winds observed by WindSat.

While WindSat cannot retrieve winds closer than 35 km from the coast, orographically induced wind systems can often be observed beyond this threshold and sometimes well out to sea (Fig. 6). High wind events south of Alaska often originate within coastal terrain gaps to produce accelerated low-level jets moving over the ocean. In Fig. 6, two major "gap winds" appear on either side of Kodiak Island (red and orange). Maximum wind speeds in each gap are about 55 kt from the north-northwest. "Safe harbor" conditions appear just south of Kodiak Island with winds at about 25 kt (green).

Conclusions: WindSat has pioneered an important new remote sensing technique for retrieving high quality winds over the world's oceans. Similar wind vector products have been available for about a decade from instruments known as scatterometers. They use an "active" strategy, whereby an onboard power supply releases periodic microwave pulses and processes the return from the ocean surface. Scatterometers have certain advantages over polarimetric instruments, including less sensitivity to precipitation and the capacity for retrievals closer to coastlines. However, the key advantage of polarimetric radiometers is that they can be used to retrieve CLW, atmospheric water vapor, and precipitation. All three are important for assessing the marine environment. In particular, CLW is crucial for assessing the accuracy of wind retrievals. Ideally, passive and active instruments can be used together to improve spatial and temporal wind vector coverage.

[Sponsored by the NOAA Joint Polar Satellite System]

References

[1] P.W. Gaiser, K.M. St Germain, E.M. Twarog, G.A. Poe, W. Purdy, D. Richardson, W. Grossman, W.L. Jones, D. Spencer, G. Golba, J. Cleveland, L. Choy, R.M. Bevilacqua, and P.S. Chang, "The WindSat Spaceborne Polarimetric Microwave Radiometer: Sensor Description and Early Orbit Performance," *IEEE Trans. Geosci. Rem. Sens.* **42**, 2347–2361 (2004).

[2] M.H. Bettenhausen, C.K. Smith, R.M. Bevilacqua, N.-Y. Wang, P.W. Gaiser, and S. Cox, "A Nonlinear Optimization Algorithm for WindSat Wind Vector Retrievals," *IEEE Trans. Geosci. Rem. Sens.* **44**, 597–610 (2006).

Atmospheric Remote Sensing Aboard the International Space Station

S. Budzien and A. Stephan
Space Science Division

Introduction: In October 2009, the Remote Atmospheric and Ionospheric Detection System (RAIDS) experiment entered science operations investigating Earth's thermosphere and ionosphere from a vantage point on the International Space Station (ISS). Built jointly by NRL and The Aerospace Corporation, RAIDS is a suite of eight limb-viewing optical sensors for remote sensing of naturally occurring airglow across the spectrum from extreme-ultraviolet to near-infrared wavelengths (55 to 870 nm). The primary objective of the RAIDS mission is to provide the first global-scale temperature measurements of the lower thermosphere. Additionally, RAIDS is serving as a pathfinder experiment for atmospheric remote sensing aboard the ISS and providing practical insights for using the ISS as a platform for future Navy remote sensing missions.

Atmospheric Observations: The RAIDS experiment is focused on the transition layer from the coldest part of the atmosphere at the mesopause near 85 km up to the hottest regions of the thermosphere above 300 km. The importance of this region connecting lower-atmospheric phenomena to the edge of space and beyond has only recently been recognized. The impact to civilian and DoD systems is well known. Changes in the ionosphere affect operational systems such as GPS navigation, radar, and radio and satellite communication. Variability in thermospheric composition, density, and winds directly affects satellite drag and space debris tracking and influences the development, structure, and variability of the ionosphere. RAIDS is addressing the paucity of global temperature measurements that are needed to cohesively couple lower-atmosphere models and their upper-atmosphere counterparts into a unified, high-accuracy space weather model that can forecast all these effects.

Airglow measured by RAIDS is produced by excitation of ambient atmospheric gas via solar radiation, charged particle precipitation, and chemical processes. Airglow measurements are interpreted using physical models of excitation and radiative transfer processes to reveal the composition, density, and temperature of the upper atmosphere. RAIDS derives thermospheric temperature from the spectral shape (color) of O_2 "atmospheric band" emission at 760 nm[1] with uncertainties nearing a few Kelvin (Fig. 7). RAIDS temperatures are in agreement with climatology estimated using the NRLMSISE-00 model.[2] In addition to this key result, RAIDS also has provided new data to enhance dayside ionospheric remote sensing techniques and to study the chemically and thermally important minor species nitric oxide.

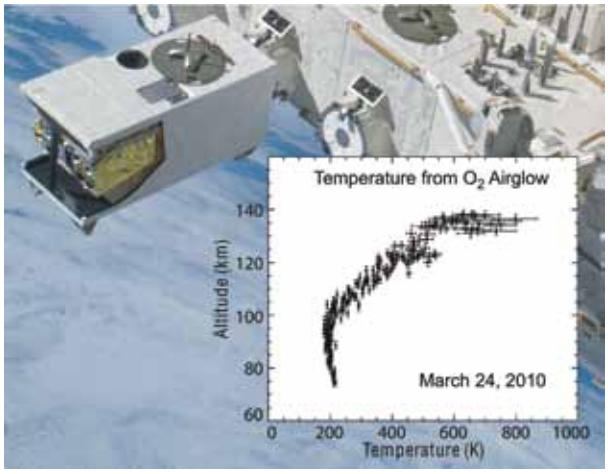

FIGURE 7
The gold-blanketed Remote Atmospheric and Ionospheric Detection System (RAIDS) experiment (top left) views the aft atmospheric limb from the open end of the HICO RAIDS Experiment Payload (HREP) aboard the International Space Station. The inset shows March 24, 2010, neutral temperatures derived from near-infrared O_2 atmospheric band emission. (Photo credit: NASA)

Mission: RAIDS and a companion experiment, NRL's Hyperspectral Imager for Coastal Ocean (HICO), comprise the HICO-RAIDS Experiment Payload (HREP) on the ISS. HREP is a collaborative venture involving the Space Science Division, the Remote Sensing Division, the Naval Center for Space Technology, and the Department of Defense Space Test Program (STP). HREP successfully demonstrated rapid, low-cost space payload development: it was designed, built, and integrated in-house at NRL facilities in only 2 years from design to delivery.

HREP is the first U.S. payload aboard the Japanese Experiment Module (JEM) Exposed Facility (EF).

On September 10, 2009, HREP was launched from Tanegashima, Japan, on the inaugural voyage of the H-IIB rocket and the H-II Transfer Vehicle (HTV), a Japanese unmanned resupply capsule for the ISS. After a week of flight maneuvers and tests, the HTV docked with the ISS. Astronauts used both the main ISS manipulator arm and a smaller arm on the JEM to transfer the modular payloads from the unpressurized section of the HTV to the JEM-EF. HREP was installed on September 24 (Fig. 8), and RAIDS entered science operations after 30 days of commissioning activities.

Using the ISS: The RAIDS team devised several strategies to maximize the science return from this unique platform. The 51.6° inclination and 340 km altitude of the ISS orbit required tailored atmospheric science objectives. Orbital precession enables observations over a range of local time and solar illumination conditions, but also requires brief monthly shutdowns as the orbital plane intersects the Sun. Extensive station structures near the field-of-regard scatter light that must be mitigated through good baffling of optical sensors. Activities aboard the manned station, including construction work and attitude perturbations from spacecraft dockings, occasionally disrupt observations. Small ISS pitch oscillations up to ±0.75° per orbit associated with solar array rotation posed a challenge for RAIDS limb measurements; NASA responded by improving the station's attitude stability. Finally, although manned environments are notoriously dirty for contamination-sensitive optical instruments, RAIDS sensors have not exhibited any unusual degradation.

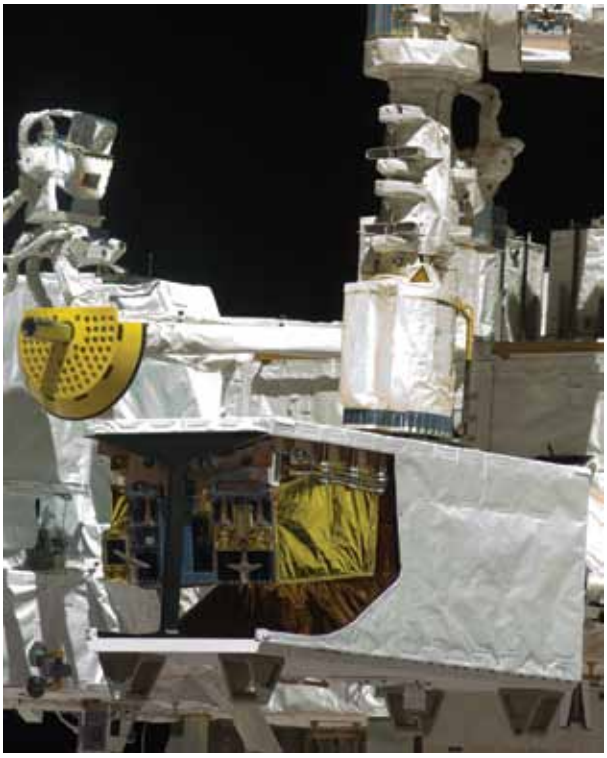

FIGURE 8
HREP (the open-ended white box) is attached to the remote manipulator arm (top) during installation onto the Japanese Experiment Module Exposed Facility. Installation and deinstallation are conducted entirely using robotic or unmanned space systems. (Photo credit: NASA)

The learning curve for developing effective mission operations was steep, as is expected for a pathfinder mission, but the RAIDS Team has met the challenge. RAIDS is functioning well and meeting its scientific objectives. The RAIDS baseline mission for 1 year could be extended up to 3 years, after which HREP will be removed from the JEM-EF and placed into an empty HTV for disposal by atmospheric reentry. By filling the gap in mid- and low-latitude temperature and composition measurements that exists in currently operating space missions, RAIDS and the ISS have combined to provide a unique, crucial dataset for studying this increasingly relevant region of the upper atmosphere.

Acknowledgments: RAIDS/HICO is integrated and flown under the direction of DoD's Space Test Program. Support for RAIDS is provided by the Office of Naval Research and The Aerospace Corporation's Independent Research and Development program.

[Sponsored by ONR and the DoD STP]

References

[1] J.W. Heller, A.B. Christensen, J.H. Yee, and W.E. Sharp, "Mesospheric Temperature Inferred from Daytime Observation of the O_2 Atmospheric (0,0) Band System," *J. Geophys. Res.* **96**(A11), 19,499–19,505 (1991).

[2] J.M. Picone, A.E. Hedin, D.P. Drob, and A.C. Aikin, "NRLMSISE-00 Empirical Model of the Atmosphere: Statistical Comparisons and Scientific Issues," *J. Geophys. Res.* **107**(A12), 1468, (2003), doi:10.1029/2002JA009430.

Geospace Climate Present and Future

J.T. Emmert
Space Science Division

Introduction: It has long been known that the near-Earth space environment responds strongly to variations in the Sun's photon, particle, and magnetic field output. More recently, it has become increasingly apparent that Earth's upper atmosphere and ionosphere are also intricately coupled to the underlying layers of the atmosphere, all the way down to the Earth's surface. It is now clear that a meaningful understanding of geospace behavior — including both climate and weather — cannot be attained except by considering the

atmosphere as a whole system that responds not only to direct solar influences, but also to internal variations and changes of both natural and anthropogenic origin. Research by NRL's Space Science Division is providing new insight into geospace climate and how it is evolving, including the atmospheric system's response to the unusual solar minimum of 2008. This research has significant implications for several applications, including policymaking to mitigate and reduce orbital debris.

Figure 9 depicts the typical structure and composition of Earth's atmosphere. The thermosphere is the operational environment of many satellites, and the

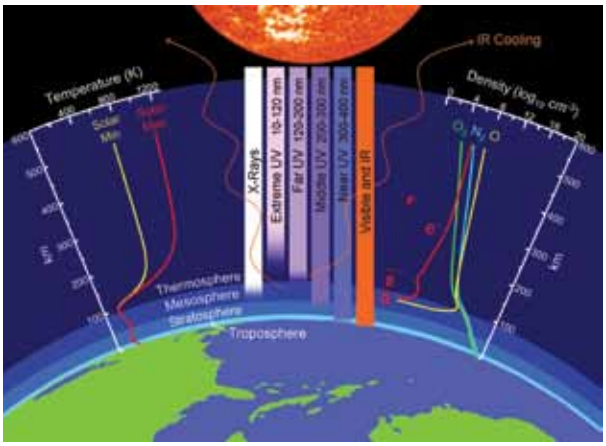

FIGURE 9
Thermal and compositional structure of Earth's atmosphere. The upper atmosphere, comprising the mesosphere, thermosphere, and embedded ionosphere, absorbs all incident solar radiation at wavelengths less than 200 nm. Most of that absorbed radiation is ultimately returned to space via infrared emissions. The plot on the left shows the typical resulting thermal structure of the atmosphere, as specified by the NRLMSISE-00 empirical model, when the flux of solar radiation is at the minimum and maximum of its 11-year cycle. The plot on the right shows the density of nitrogen (N_2), oxygen (O_2), and monatomic oxygen (O), the three major neutral species in the upper atmosphere, along with the free electron (e^-) density (from the International Reference Ionosphere), which is equal to the combined density of the various ion species. The F, E, and D layers of the ionosphere are also indicated.

embedded ionosphere is an electric medium that fundamentally affects the propagation of radio-frequency communication and navigation signals. This region of the atmosphere is heated and ionized primarily via absorption of solar extreme ultraviolet (EUV) radiation; at high latitudes, energetic particles of solar origin and resistive dissipation of magnetospheric currents are also significant energy sources. Solar EUV irradiance increases by a factor of 2 from the minimum to maximum of an 11-year solar cycle, and the thermosphere responds by heating and expanding. The orbital drag experienced by satellites consequently varies drastically over a solar cycle, as illustrated in Fig. 10.

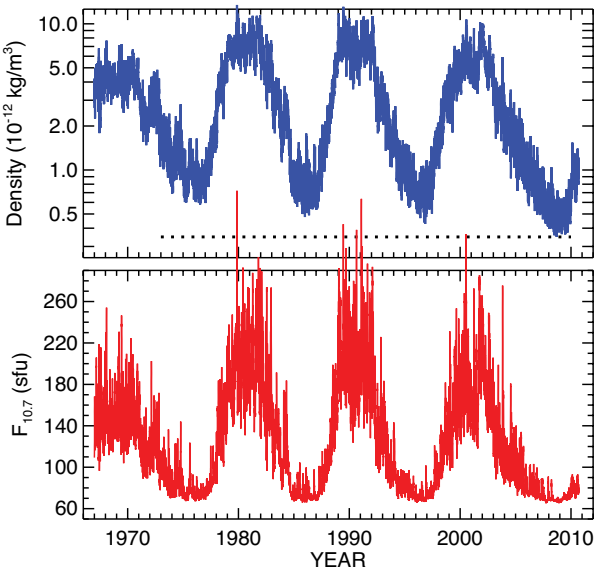

FIGURE 10
(Top) Global-average mass density, derived from the orbits of ~5000 objects, at an altitude of 400 km. The dotted horizontal line indicates the minimum overall density. (Bottom) The daily 10.7 cm solar radio flux ($F_{10.7}$) normalized to 1 AU, in solar flux units (sfu, 10^{-22} W m^{-2} Hz^{-1}). $F_{10.7}$ is a proxy for solar extreme ultraviolet irradiance.

Changing Geospace Climate: The same gases that have been implicated in lower atmospheric climate change also play important roles in the energy balance of the upper atmosphere. CO_2 is the primary cooling agent of the upper mesosphere and thermosphere (where, unlike in the troposphere, the atmosphere is too thin optically to trap infrared radiation emitted by CO_2). Anthropogenic increases in CO_2 propagate into the upper atmosphere, and there are strong theoretical grounds and experimental evidence[1,2] that these increases are causing the upper atmosphere to cool and contract. Some of the changes predicted to occur as a result of greenhouse gas increases have been detected in historical upper atmospheric data, and a coherent picture is beginning to emerge[2,3] (Fig. 11). NRL has contributed significantly to the study of geospace climate change by analyzing the orbital decay rates of thousands of low-Earth-orbit (LEO) objects covering the past 40 years; the results indicate that, after accounting for solar influences, thermospheric density at fixed heights has been decreasing at a rate of 2% to 5% per decade.[4]

There are also natural sources of geospace climate change. Long-term variations in the Sun's photon, particle, and magnetic field output will directly affect the structure and climate of the upper atmosphere. Secular changes in the geomagnetic field will further alter the distribution of plasma and the location and intensity of ionospheric currents. Because the state of the upper atmosphere responds strongly to solar drivers, both an-

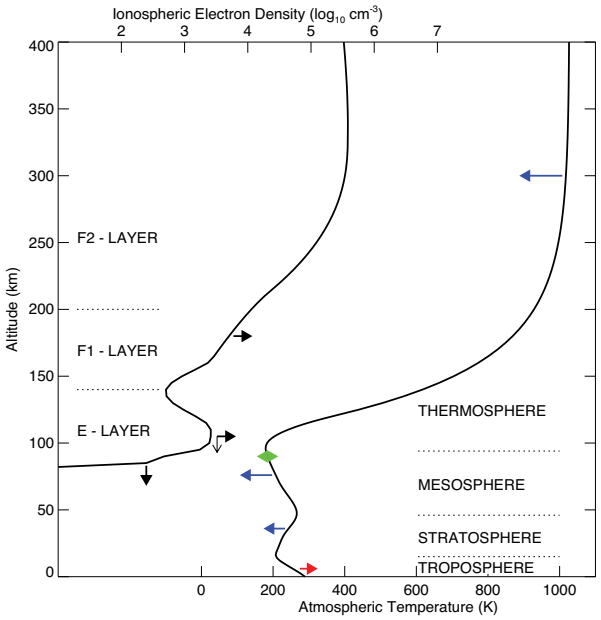

FIGURE 11

Qualitative summary of observed long-term trends in the atmosphere and ionosphere. Orbital drag studies at NRL and other institutions indicate a decrease in thermospheric temperature. A large body of research demonstrates temperature increases in the lower troposphere, decreases in the stratosphere and mesosphere, and no significant change near the mesopause (the boundary between the mesosphere and thermosphere). Electron densities in the E and F1 layers of the ionosphere have increased, and the heights of the E layer and the bottomside ionosphere have lowered. This qualitative picture is consistent with the predicted effects of CO_2 and O_3 changes in the atmosphere.

thropogenic and natural climate changes of terrestrial origin will, to varying degrees, depend on the phase of the solar cycle. Conversely, any terrestrial-driven climate change is expected to alter how the upper atmosphere responds to solar variations.

The exceptionally quiescent 2008 solar minimum, which had the greatest number of days without sunspots since the 1933 minimum, has provided a valuable opportunity to better understand this interplay between solar and lower atmospheric influences on geospace climate. An initial NRL study determined that thermospheric mass density was lower in 2008 than at any time since the beginning of the Space Age, and 30% lower than during the previous solar minimum[5] (see Fig. 10). The unusually quiet Sun can account for some of this reduction, as can record-high levels of atmospheric CO_2, but the state of the thermosphere during the past few years is still poorly understood and is an active research topic at NRL and other institutions. Besides contributing to the unusual behavior of the thermosphere, the quietness of the Sun has also facilitated discovery of previously unrecognized connections between the lower atmosphere and the space environment; in one such connection, dynamical events in the polar stratosphere can alter the electron content of the low-latitude ionosphere by up to 100%.[6]

Implications for Orbital Debris: The anthropogenic and natural evolution of geospace climate will have a profound effect on the LEO debris population because atmospheric drag is currently the only effective mechanism by which debris is removed from orbit. Of the 16,000 objects in the active satellite catalog (which only includes objects larger than 10 cm), 12,000 are debris or expended rocket bodies. The greatest density of debris is found between 500 and 1100 km altitude, where removal by atmospheric drag can take from 25 years to centuries. Recent studies have found that even without any new launches, the amount of debris in LEO will increase via collisional fragmentation faster than it is removed from orbit by atmospheric drag.[7] Active debris removal (ADR) strategies are therefore being explored by the international space community, but it is not clear how geospace climate change may affect these strategies. An initial study by researchers at the University of Southampton suggests that when potential long-term contraction of the thermosphere is taken into account, the effectiveness of ADR is dramatically reduced, thereby increasing the costs of achieving a stable debris population within the next hundred years.[8] In addition to long-term contraction, anomalous reductions in thermospheric density, such as occurred unexpectedly during the recent solar minimum, may also adversely affect efforts to control debris growth.

[Sponsored by ONR and NASA]

References

[1] R.G. Roble and R.E. Dickinson, "How Will Changes in Carbon Dioxide and Methane Modify the Mean Structure of the Mesosphere and Thermosphere?" *Geophys. Res. Lett.* **16**, 1441–1444 (1989).

[2] J. Laštovička, R.A. Akmaev, G. Beig, J. Bremer, J.T. Emmert, C. Jacobi, M.J. Jarvis, G. Nedoluha, Y.I. Portnyagin, and T. Ulich, "Emerging Pattern of Global Change in the Upper Atmosphere and Ionosphere," *Ann. Geophys.* **26**, 1255–1268 (2008).

[3] J. Laštovička, R.A. Akmaev, G. Beig, J. Bremer, and J.T. Emmert, "Global Change in the Upper Atmosphere," *Science* **314**, 1253–1254 (2006).

[4] J.T. Emmert, J.M. Picone, and R.R. Meier, "Thermospheric Global Average Density Trends, 1967–2007, Derived from Orbits of 5000 Near-Earth Objects," *Geophys. Res. Lett.* **35**, L05101 (2008), doi:10.1029/2007GL032809.

[5] J.T. Emmert, J.L. Lean, and J.M. Picone, "Record-Low Thermospheric Density during the 2008 Solar Minimum," *Geophys. Res. Lett.* **37**, L12102 (2010), doi:10.1029/2010GL043671.

[6] L.P. Goncharenko, A.J. Coster, J.L. Chau, and C.E. Valladares, "Impact of Sudden Stratospheric Warmings on Equatorial Ionization Anomaly," *J. Geophys. Res.* **115**, A00G07 (2010), doi:10.1029/2010JA015400.

[7] J.-C. Liou and N.L. Johnson, "Instability of the Present LEO Satellite Populations," *Adv. Space Res.* **41**, 1046–1053 (2008).

[8] H.G. Lewis, A. Saunders, G. Swinerd, and R. Newland, "Understanding the Consequences of a Long-Term Decline in Thermospheric Density on the Near-Earth Space Debris Environment," 6th IAGA/ICMA/CAWSES Workshop on Long-Term Changes and Trends in the Atmosphere, Boulder, Colorado, June 2010.